Molecular Electronics

International Edition: DOI: 10.1002/anie.201505447
German Edition: DOI: 10.1002/ange.201505447

Single-Molecule Spin Switch Based on Voltage-Triggered Distortion of the Coordination Sphere

Gero D. Harzmann, Riccardo Frisenda, Herre S. J. van der Zant, and Marcel Mayor**

Abstract: *Here, we report on a new single-molecule-switching concept based on the coordination-sphere-dependent spin state of Fe^{II} species. The perpendicular arrangement of two terpyridine (tpy) ligands within heteroleptic complexes is distorted by the applied electric field. Whereas one ligand fixes the complex in the junction, the second one exhibits an intrinsic dipole moment which senses the E field and causes the distortion of the Fe^{II} coordination sphere triggering the alteration of its spin state. A series of complexes with different dipole moments have been synthesized and their transport features were investigated via mechanically controlled break-junctions. Statistical analyses support the hypothesized switching mechanism with increasing numbers of junctions displaying voltage-dependent bistabilities upon increasing the Fe^{II} complexes' intrinsic dipole moments. A constant threshold value of the E field required for switching corroborates the mechanism.*

The vision of profiting from the small dimensions and the structural diversity of single molecules as functional units in electronic circuits was first expressed by Aviram and Ratner in their ground-breaking paper dealing with a hypothetical molecular rectifier.[1] The concept of integrating molecules to tune the electronic function of a device had been formulated previously by Hans Kuhn with his vision of "molecular engineering".[2] Numerous experiments reporting transport studies through single molecules appeared since then and various electronic features such as conductivity and rectification have been correlated with the molecules' structures.[3–7] A particularly interesting function on a molecular level is the switching between two transport states, as a molecule with the behavior also holds the potential to act as a minute memory unit.[8,9] The application of external stimuli to trigger the switch is usually a difficult problem at the single-molecule level and in many cases, the triggering signal is considerably larger than the molecular junction (e.g. light,[10] gating electrode,[11] electrochemical potential[12]). Particularly appealing would be molecular junctions that respond to the applied voltage or current and thus do not require an additional contact. Apart from the simplest molecular switch working like a fuse, reversible bias-dependent switching in molecular junctions is rarely reported and the underlying switching mechanism is often not fully understood. Examples are the dinitrobipyridine-based structures developed by Tour and co-workers[13] and the negative differential resistance (NDR) junction reported by Reed and co-workers.[14]

Here, we present a new concept of bias-dependent switching in molecular junctions based on spin crossover (SCO) coordination compounds. Single-molecule junctions with electrostatic-field-dependent SCO phenomena have been suggested theoretically[15] and real molecular junctions with spin states that are switched electrically have been demonstrated in low-temperature scanning tunneling microscopy (STM) experiments using Fe-phen complexes either in bilayers[16] or decoupled from the substrate by a thin insulating layer.[17] Spin crossover complexes have been investigated on surfaces in various concentrations ranging from submonolayers[18] to thin films.[19–21] They have been integrated as functional components in nanocrystals,[22] in arrays of nanoparticles,[23] in multilayer architectures,[24] and in bulk materials as mechanically interlocked building blocks[25] and as mechanical pressure sensors.[26] The integration of SCO compounds on various levels has been reviewed[27,28] together with theoretical considerations.[29] Also single-molecule junctions comprising metal terpyridine (tpy) or structurally related complexes are known, like for example, Kondo studies with Fe andr Co complexes[30,31] or a Ru complex acting like a cardan-joint structural element.[32]

In this paper the single-molecule switching mechanism is based on the sensitivity of the spin states of $[Fe^{II}(tpy)_2]$ complexes to the spatial arrangement of the ligands and is sketched in Figure 1. The octahedral coordinated Fe^{2+} ion results in five spin-degenerate levels. In an almost perfect octahedral coordination sphere the crystal field interaction is strong enough to pair up all the electrons giving the low-spin (LS) ground state with zero net spin ($S = 0$). By reduction of the crystal field interaction, for example, by increasing the metal–ligand distance through mechanical distortion of the coordination sphere, the crystal field splitting parameter Δ_{oct} decreases and the e_g states become accessible. Filling the

[*] Dr. G. D. Harzmann,[+] Prof. Dr. M. Mayor
Department of Chemistry, University of Basel
St. Johanns-Ring 19, 4056 Basel (Switzerland)
E-mail: marcel.mayor@unibas.ch
Prof. Dr. M. Mayor
Institute for Nanotechnology (INT)
Karlsruhe Institute of Technology (KIT)
P.O. Box 3640, 76021 Karlsruhe (Germany)
and
Lehn Institute of Functional Materials (LIFM)
Sun Yat-Sen University (SYSU), Guangzhou (China)
R. Frisenda,[+] Prof. Dr. H. S. J. van der Zant
Kavli Institute of Nanoscience
Department of Quantum Nanoscience
Delft University of Technology
P.O. Box 5046, 2600 GA Delft (The Netherlands)
E-mail: h.s.j.vanderzant@tudelft.nl
[+] These authors contributed equally to this work.

Supporting information for this article is available on the WWW under http://dx.doi.org/10.1002/anie.201505447.

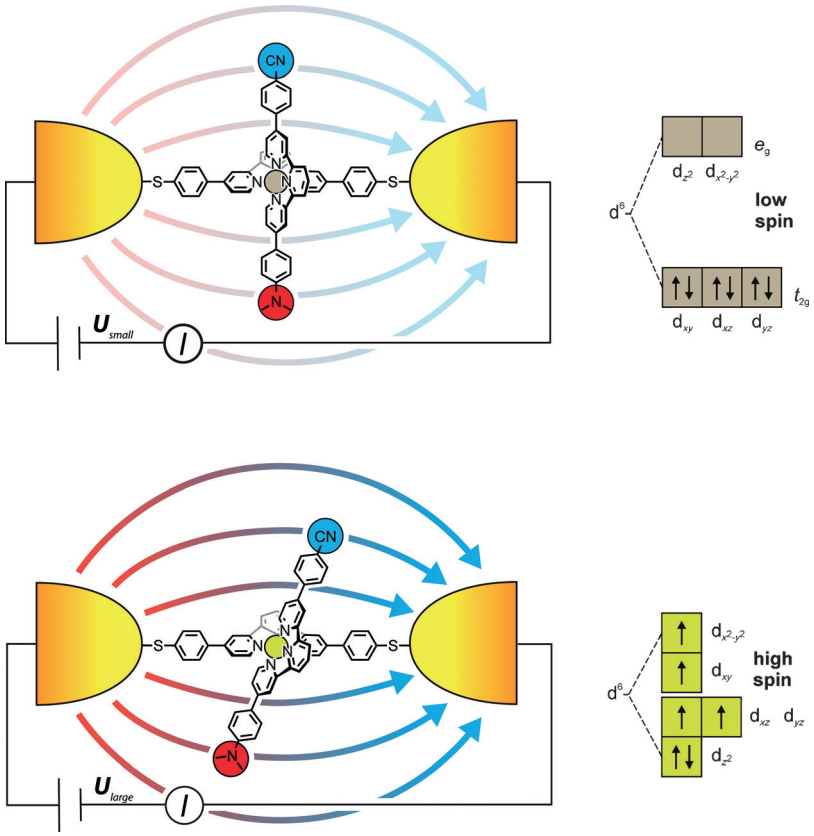

Figure 1. Idealized sketch of the voltage-triggered spin crossover switch in a single-molecule junction. Top: Low-spin Fe^{II} complex **1** bridging the two electrodes at a small applied voltage. Bottom: High-spin Fe^{II} complex **1** with distorted coordination sphere due to the alignment of the push–pull system in the applied electric field.

levels according to Hund's rule leads to a maximization of the total net spin (S = 2), the so-called high-spin (HS) state.[33,34] In an octahedral $[Fe^{II}(tpy)_2]$ complex the two tpy ligands are perpendicular to each other.[35] The molecular design of the SCO switch is thus based on a heteroleptic $[Fe^{II}(tpy)_2]$ complex in which one tpy ligand is functionalized with terminal anchor groups to fix the molecule inside the junction and the other tpy ligand exhibits a push–pull system responding to the strength of the applied electric field.

An idealized representation of the intended switching of a freely suspended complex between the two electrodes is displayed in Figure 1. The top part of Figure 1 shows the immobilized complex with a perpendicular arrangement of the two tpy ligands in the LS state. When the applied voltage is increased, the electric field inside the junction increases, bending the second tpy ligand out of its perpendicular arrangement and thereby distorting the octahedral ligand field. Thus at a given threshold voltage, the Fe^{2+} ion is expected to switch to its HS state. Due to the 4,4″-disubstitution pattern at the core of the tpy ligand bridging the electrodes, the current passes through the Fe^{2+} ion and its alteration in spin states should be reflected in the junction's transport characteristics.

According to theoretical predictions[36] and low-temperature STM experiments,[17] the HS state is assumed to be the better conducting one. These hypotheses on the expected current alterations are, however, affected by the limited control over the spatial arrangement of the complex immobilized in the break junction, resulting in an uncertainty concerning the initial spin state. In order to compensate for the intrinsic diversities of real single-molecule junctions emerging from variations of the spatial arrangement of the terminal metal atoms of the electrodes as well as the immobilized molecule(s),[37,38] a series of complexes with varying dipole moments was investigated to trace the expected SCO phenomenon in a structure–property correlation approach.

Several heteroleptic complexes comprising either an SCO-active central $[Fe^{II}(tpy)_2]$ subunit (**1**–**4**) and a dipole moment of various strengths in the tpy ligand or the SCO-silent central $[Ru^{II}(tpy)_2]$ subunit in **5** were synthesized (Scheme 1). All tpy ligands were assembled by Suzuki–Miyaura cross-coupling reactions and share 4,4″-dichloroterpyridine (**6**) as a common precursor. As previously reported,[39] the chlorine atoms of **6** can be substituted efficiently by aryl boronic acid derivatives using an optimized Pd-based catalytic system.[40] The assembly of the 4,4″-*para*-acetylsulfanylphenylterpyridine **12** via the trimethylsilylethynyl-masked precursor **11** was already reported.[39]

For the assembly of the push–pull tpy ligands **14**–**16** a statistical coupling strategy was applied. The dichloro tpy precursor **6** was exposed to substoichiometric amounts of the aryl boronic acid derivative and, considering the statistical nature of the reaction, the monofunctionalized tpys **7**–**10** were isolated in very good yields. The remaining starting material could be recovered, further increasing the appeal of the statistical strategy. The second chlorine atom was substituted in excellent yields by applying similar coupling conditions but using an excess of the aryl boronic acid derivative. Slightly better yields were obtained when the electron-donating substituent was introduced first, as displayed with push–pull ligands **14** and **16** which were synthesized in both ways.

With all tpy ligands in hand, the heteroleptic Fe^{II} complexes **1**–**4** were synthesized again in a statistical approach. Equimolar amounts of both ligands and $FeCl_2$ were dissolved in a methanol/dichloromethane mixture, diluted with water, and precipitated with NH_4PF_6. The mixture of $[Fe^{II}(tpy)_2]$ complexes was collected quantitatively as a dark purple precipitate. Analysis by electrospray ionization mass spectrometry (ESI-MS) revealed the expected statistical mixtures with the desired heteroleptic complex and the two homoleptic complexes in a ratio of 2:1:1. The Ru^{II} complex **5** was synthesized with a similar statistical strategy, using $RuCl_3 \cdot (x\,H_2O)$ as the ruthenium source in an ethanol/chloroform mixture and precipitating with NH_4PF_6 after refluxing with *N*-ethylmorpholine. Small but analytically pure

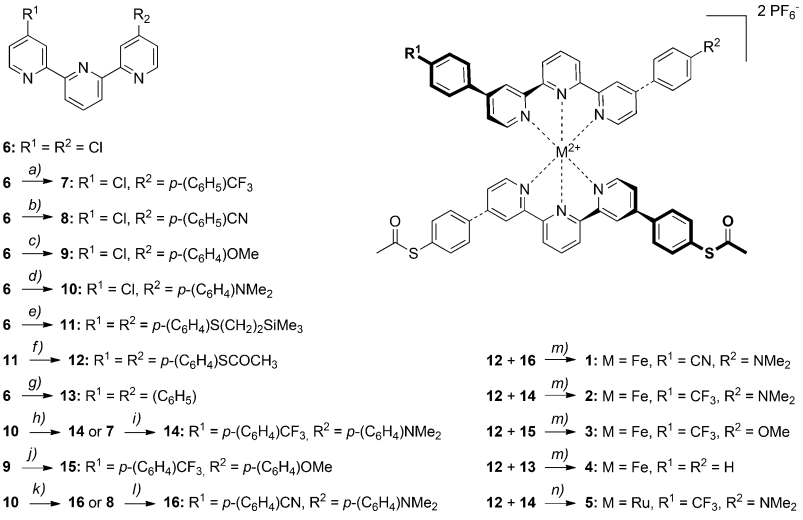

Scheme 1. Syntheses of the heteroleptic Fe^{II} complexes **1**–**4** and the Ru^{II} complex **5**, together with the syntheses of their ligands. Reagents and conditions: general catalytic system (gcs): K_2CO_3, $[PdCl_2\{PtBu_2(p\text{-}NMe_2\text{-}Ph)\}_2]$, $C_6H_5CH_3/H_2O$ (6:1 or ratio cited), reflux, 24 h; a) p-$CF_3C_6H_4B(OH)_2$ (0.75 equiv), gcs, 44%; b) p-$NC\text{-}NC_6H_4B(OH)_2$ (0.75 equiv), gcs, 26%; c) p-$CH_3OC_6H_4B(OH)_2$ (2 equiv), gcs, 42%; d) p-$(CH_3)_2NC_6H_4B(OH)_2$ (5.51 equiv), gcs, 58%; e) $(p\text{-}(CH_3)_3Si(CH_2)_2SC_6H_4BO)_3$ (2 equiv), gcs, $C_6H_5CH_3/H_2O$ (5:1), 99%; f) THF, TBAF (10 equiv), AcCl (200 equiv), RT to −10°C, 3.5 h, 96%; g) $C_6H_5B(OH)_2$ (10 equiv), gcs, $C_6H_5CH_3/H_2O$ (4:1), quant.; h) p-$CF_3C_6H_4B(OH)_2$ (3 equiv), gcs, quant.; i) p-$(CH_3)_2NC_6H_4B(OH)_2$ (10 equiv), gcs, quant.; j) p-$CF_3C_6H_4B(OH)_2$ (10 equiv), gcs, $C_6H_5CH_3/H_2O$ (5:1), quant.; k) p-$NC\text{-}C_6H_4B(OH)_2$ (9.51 equiv), gcs, 94%; l) p-$(CH_3)_2NC_6H_4B(OH)_2$ (10 equiv), gcs, $C_6H_5CH_3/H_2O$ (5:1), 92%; m) 1. $FeCl_2$, CH_3OH, CH_2Cl_2; 2. H_2O; 3. NH_4PF_6, 50°C, ca. 50% (quant. as 2:1:1 mixture); n) 1. $RuCl_3\cdot(xH_2O)$, C_2H_5OH, $CHCl_3$, reflux; 2. *N*-ethylmorpholine, reflux; 3. NH_4PF_6, reflux, ca. 50% (quant. as 2:1:1 mixture).

samples of all four heteroleptic Fe^{II} complexes **1**–**4** and the Ru^{II} complex **5** were obtained by preparative HPLC from the corresponding reaction mixtures. The complexes were fully characterized by ^1H and ^{13}C NMR spectroscopy, UV spectroscopy, and high-resolution mass spectrometry.

Single-molecule-transport investigations were performed in a mechanically controlled break junction (MCBJ) setup. The concept of the MCBJ experiment is sketched in Figure 2 and described in detail in the Supporting Information. In short, when the substrate with a lithographically fabricated suspended gold structure on top is bent, the ductile nature of the metal enables the elongation of the bridge (I in Figure 2) until its rupture. As a result the two extremities face each other and act as a pair of nanoelectrodes (II in Figure 2). The flexible substrate allows the approach of the two extremities by adjusting the bending tension. In the experiments presented here, the MCBJ sample was first immersed for 5 h in a freshly prepared 0.5 mM solution of the complex under investigation in acetonitrile at room temperature.[41] The complex-decorated gold sample was subsequently mounted in the bending setup and connected to the electronic circuit before the entire experiment chamber was evacuated to 10^{-7} mbar and cooled to liquid-helium temperature. During the rupture process a molecule can bridge the formed nanoelectrodes, enabling transport measurements through the molecule (III in Figure 2). The stability of the setup makes it possible to stay at the single-molecule bridging level and to investigate the response of the molecular junction on the variation of the applied voltage (IV in Figure 2).

With complexes **1**–**5**, large enough numbers (293–758) of junctions were formed such that their voltage-dependent behavior could be analyzed statistically. The behavior of the junctions can be divided into three types, which are discussed using the Fe complex **1** as a representative example. The first type are empty junctions lacking a bridging molecule after rupture of the gold electrodes. Of the 293 junctions formed, 224 (76%) displayed an exponential decay of the current with increased electrode spacing, which is the typical behavior of an empty pair of gold electrodes. The remaining 69 (24%) junctions display conductance plateaus more than two orders of magnitude below the conductance of a single Au atom ($G_0 = 2e^2/h$) indicative of a bridging molecule. Of these junctions 28 (9.6% of all junctions or 41% of the junctions comprising a molecule) belong to the second type displaying voltage-dependent bistability features, while 41 junctions are of the third type where no bistabilities were observed in their *I*–*V* plots. Interestingly, a variety of bistability features were observed which are displayed in Figure 3. Of the 28 junctions of **1** exhibiting bistability, four display a clearly pronounced hysteresis window around the switching point. A typical *I*–*V* curve is displayed in Figure 3a) where the current jumps to a lower value at a positive bias of 0.7 V and upon sweeping in the opposite direction, the high current state is re-established at −0.5 V. The remaining 24 junctions express their bistabilities either by negative differential conductance (NDC) features (Figure 3b) or by sudden jumps to different current states (Figure 3c). The NDC example of Figure 3b has a pronounced dip in the current at a bias around −0.5 V, and a representative example of a jump to a different current state is displayed in Figure 3c with a pronounced step at −1 V and different *I*–*V* slopes on either side of the step. In contrast to the hysteretic features, the NDC and the jumps are reproducibly observed in both sweep directions (blue and red in Figure 3b,c). Considering the large diversity of possible arrangements of the complex in the junction with various extents of interactions with the electrodes' surface, the variation of the characteristics of the molecular junctions in general, and of the observed bistability features in particular is not surprising.

Interestingly none of the observed bistable *I*–*V* plots fulfill the expectation for the ideal case of a freely suspended complex as sketched in Figure 1, but rather point to more complex geometries that probably also comprise molecule–electrode interactions. Possible atomistic realizations of molecular junctions leading to the observed bistable *I*–*V* curves are displayed in the Supporting Information (Figures S1–S3). The variation makes the analysis of the SCO-based

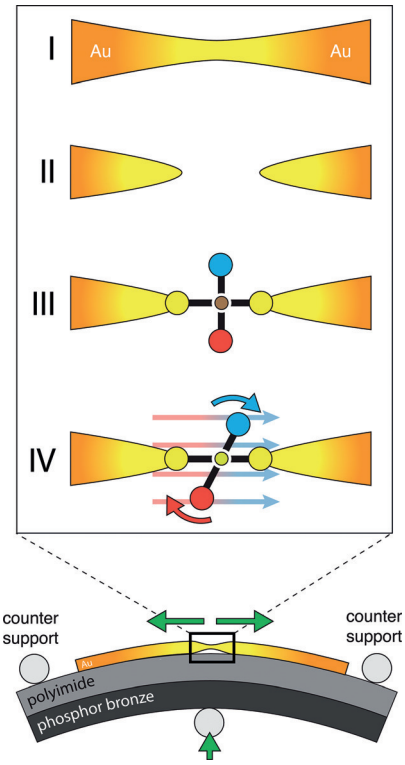

Figure 2. Bottom: Schematic illustration of a mechanically controllable break junction (MCBJ) setup. Top: Four different stages of the experiment: I) Stretching of the Au wire until II) its rupture. III) Metal complex bridging the two electrodes and IV) manipulation of the spatial arrangement of the complexes' ligands upon application of an electric field.

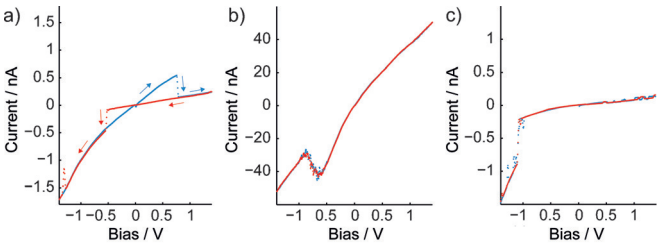

Figure 3. Variation of *I*–*V* plots displaying bistabilities (forward bias sweep: blue; backward sweep: red): a) hysteresis, b) NDC, and c) jump in current.

phenomenon more challenging and to extract statistically relevant trends from the data we performed extended series of control experiments. To correlate the presence of the metal in the complex as the origin of the bistability, similar molecular junctions were assembled with an organic rigid rod-type OPE molecule of comparable dimensions exhibiting the same terminal anchor groups (OPE in Figure 4). In the 856 rupture experiments a comparable ratio of 65 junctions (7%) contained a molecule. None of these 65 junctions displayed bistability features supporting the hypothesis that the observed bistability emerges from the SCO complex.

To further substantiate the voltage-triggered distortion of the ligands, we investigated junctions with $[Fe^{II}(tpy)_2]$ complexes **1**–**4** which cover a range of intrinsic dipole moments. While **4** has no dipole moment in the second tpy ligand, the dipole moment increases in the series from **3** to **2** and **1**. If the hypothesized mechanism applies, these differences should be reflected in the statistics of the junctions' *I*–*V* characteristics. These studies were complemented by the $[Ru^{II}(tpy)_2]$ complex **5** whose dipole moment is as strong as that of **2**. As **5** does not exhibit SCO phenomena, it is a valuable model compound to identify bistabilities arising from the molecular shape and/or interactions with the electrodes and not from a voltage-triggered SCO in the central metal ion. The results of these extended studies are graphically summarized in Figure 4.

The pie charts in Figure 4 display for each compound the proportion of junctions comprising an immobilized molecule. The ratios vary from 6% to 25% but we were not able to correlate these numbers to particular structural parameters of the molecules. For the molecular junctions formed with **2** and **5**, which differ solely in their central metal ion, the significant difference in the ratio clearly shows that the experimental data are not suited to draw conclusions about the molecule's structure. The lower row in Figure 4 shows the ratio of molecular junctions displaying bistabilities. A clear trend can be seen: the relative proportion of junctions exhibiting bistability increases with the strength of the dipole moment and the presence of the central Fe^{2+} ion. While not a single junction displaying bistability was found for the organic OPE rod, also the Ru^{II} complex **5** without a SCO-compatible central ion and the Fe^{II} complex **4** without a perpendicular dipole moment formed some bistable junctions. Even though these ratios are small, the fact that such junctions are observed suggests that there are mechanisms beyond the present voltage-triggered ligand distortion with concomitant SCO which might result in bistable junctions as well. While in the case of the Fe^{II} complex **4** the tpy ligand might align in the electric field due to its polarizability, the bistabilities observed for the Ru^{II} complex **5** cannot be related to a SCO of the central ion. Besides this rather surprising finding, the series of Fe^{II} complexes **3** to **1**, with bistable junction ratios of 2.6%, 3.3%, and 9.6% that correlate with the complexes' dipole moments, supports the hypothesis of an *E*-field-triggered SCO.

In order to further scrutinize the hypothesized switching mechanism, all bistable *I*–*V* plots of the junctions with the Fe^{II} complex **1** were analyzed (similar analyses of complexes **2** and **3** are shown in the Supporting Information). The histogram in Figure 5a displays the applied bias at which switching was observed summed up over all junctions. Two maxima, one at negative and one at positive bias, are observed representing a typical absolute switching voltage for junctions of **1** between 0.25 and 1.5 V. The larger number of events on the left-hand side may arise from statistical fluctuations owing to the limited number of data points. Apart from that difference in numbers, the two peaks are symmetric as expected for the hypothesized mechanism which should not particularly favor one direction over the other.

Finally the switching mechanism was investigated on the single-junction level, profiting from the sharp features of a junction bridged by complex **1** that displayed hysteretic switching. In the intended switching mechanism the push–pull

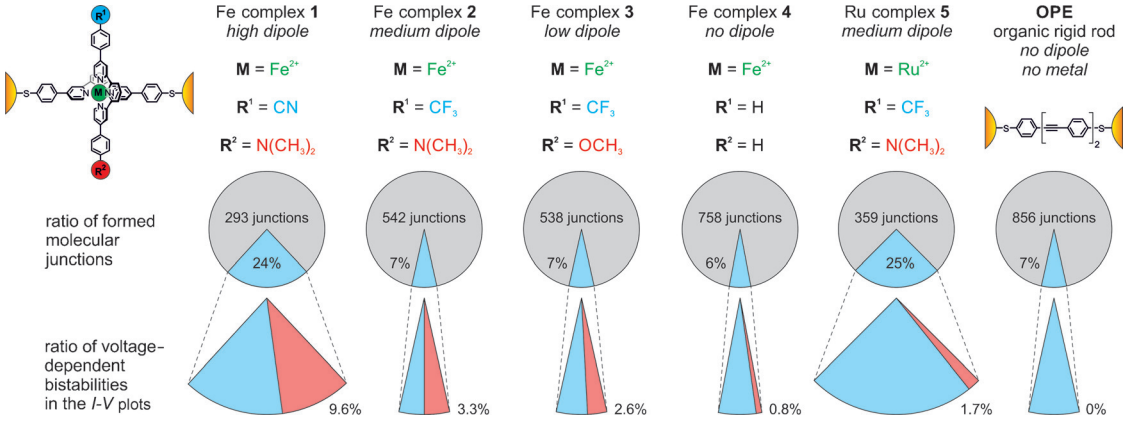

Figure 4. Statistical analysis of the MCBJ experiments with the heteroleptic metal complexes **1**–**5** and the metal-free rigid rod OPE. The pie charts in the upper row display in blue the probability of finding a molecule immobilized in the MCBJ; in the lower row the sections in red represent the ratio of molecular junctions displaying bistability features in their *I*–*V* curves.

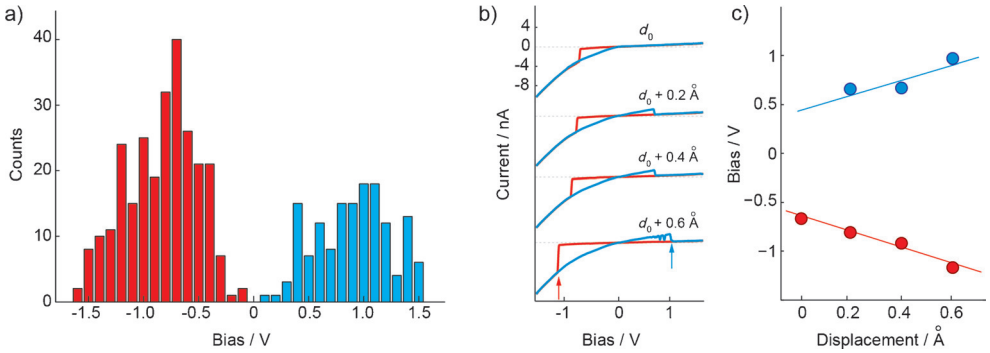

Figure 5. Analysis of bistable junctions formed by the Fe^{II} complex **1**. a) Histogram of the switching bias voltage for all *I*–*V* plots of **1** displaying bistability features. b) Current–voltage characteristics for increasing electrode separation showing a hysteretic switching behavior. The curves are offset in the vertical direction for clarity. The red and blue arrows indicate the switching points for the electrode spacing $d_0 + 0.6$ Å. c) Switching bias voltage as a function of electrode separation for the *I*–*V* data of (b). The solid red and blue lines are guides for the eye and display the linear relationship.

system of the tpy ligand senses the applied electric field. While the threshold voltage triggering the switching between the two spin states might vary slightly from junction to junction due to different arrangements of the electrodes and the bridging molecule, it should remain constant in a given junction. One of the most appealing features of the MCBJ experiment is that the electrode spacing can be slightly altered without losing the bridging molecule. This is in particular the case because molecular junctions are often formed with molecules that are not fully stretched out initially, but rather connect two electrodes in a skewed arrangement. Thereby starting at a given initial molecular junction with electrode spacing d_0, there is considerable room for further separation of the electrodes without losing the bridging molecule. The electric field E inside the junction then correlates linearly with the applied voltage U divided by the electrode spacing d ($E = U/d$). Thus the threshold voltage required to trigger the SCO in the immobilized complex should increase linearly with d. The inspection of a bistable junction of **1** is displayed in Figures 5b,c. The conductance jumps are determined as a function of electrode displacement and indeed, the voltage required to trigger the jump increases in both bias directions linearly with a very similar slope (red and blue lines in Figure 5c). The linear relationship between electrode spacing and required voltage to trigger the bistability corroborates a constant threshold value for the E field required for the switching event in a given junction and further supports the hypothesized switching mechanism.

In summary, a new single-molecule switching concept relying on the E-field-dependent coordination sphere of Fe^{II} terpyridine complexes has been investigated with model compounds having various dipole moments in a MCBJ setup in vacuum at liquid-helium temperature. In spite of the large diversity of recorded *I*–*V* plots, a series of model compounds in combination with a large number of investigated junctions were used to relate bistabilities in the *I*–*V* curves with the complexes' dipole moments which distort the coordination sphere in the E field. This finding supports the hypothesized SCO switching mechanism. Detailed inspection of an individual junction further corroborated the mechanism because a constant E field was found to be required to trigger the junction.

While this phenomenological paper displays experimental data analyzing the hypothesized switching concept, we hope also that it will serve as inspiration for a more detailed theoretical investigation of the phenomenon. We are currently working on single-molecule SCO junctions that respond to alternative triggers like for example, mechanically and optically addressed systems.

Acknowledgements

We acknowledge financial support by the European FP7-ITN network MOLESCO, the Swiss National Science Foundation (SNF), the Dutch funding agencies NWO/OCW and FOM, and an ERC advanced grant (Mols@Mols). We thank Michel Rickhaus for his graphical support with the figures displayed throughout this manuscript. We further thank Dr. B. Wagner, Novartis, and Dr. M. Neuburger, University of Basel, for data collection, structure solution, and refinement of the X-ray structures displayed in the Supporting Information.

Keywords: break junction · Fe terpyridine · molecular electronics · molecular switches · spin crossover

How to cite: *Angew. Chem. Int. Ed.* **2015**, *54*, 13425–13430
Angew. Chem. **2015**, *127*, 13624–13630

[1] A. Aviram, M. A. Ratner, *Chem. Phys. Lett.* **1974**, *29*, 277–283.
[2] H. Kuhn, D. Möbius, *Angew. Chem. Int. Ed. Engl.* **1971**, *10*, 620–637; *Angew. Chem.* **1971**, *83*, 672–690.
[3] J. R. Heath, M. A. Ratner, *Phys. Today* **2003**, *56*, 43–49.
[4] C. Joachim, J. K. Gimzewski, A. Aviram, *Nature* **2000**, *408*, 541–548.
[5] K. Moth-Poulsen, T. Bjørnholm, *Nat. Nanotechnol.* **2009**, *4*, 551–556.
[6] N. Weibel, S. Grunder, M. Mayor, *Org. Biomol. Chem.* **2007**, *5*, 2343–2353.
[7] A. H. Flood, J. F. Stoddart, D. W. Steuerman, J. R. Heath, *Science* **2004**, *306*, 2055–2056.
[8] N. Fuentes, A. Martín-Lasanta, L. Á. de Cienfuegos, M. Ribagorda, A. Parra, J. M. Cuerva, *Nanoscale* **2011**, *3*, 4003–4014.
[9] S. J. van der Molen, P. Liljeroth, *J. Phys. Condens. Matter* **2010**, *22*, 133001.
[10] D. Dulić, S. van der Molen, T. Kudernac, H. Jonkman, J. de Jong, T. Bowden, J. van Esch, B. Feringa, B. van Wees, *Phys. Rev. Lett.* **2003**, *91*, 207402.
[11] E. A. Osorio, T. Bjørnholm, J.-M. Lehn, M. Ruben, H. S. J. van der Zant, *J. Phys. Condens. Matter* **2008**, *20*, 374121.
[12] S. Guo, J. M. Artés, I. Díez-Pérez, *Electrochim. Acta* **2013**, *110*, 741–753.
[13] E. Lörtscher, J. W. Ciszek, J. Tour, H. Riel, *Small* **2006**, *2*, 973–977.
[14] J. Chen, M. A. Reed, A. M. Rawlett, J. M. Tour, *Science* **1999**, *286*, 1550–1552.
[15] N. Baadji, M. Piacenza, T. Tugsuz, F. D. Sala, G. Maruccio, S. Sanvito, *Nat. Mater.* **2009**, *8*, 813–817.
[16] T. G. Gopakumar, F. Matino, H. Naggert, A. Bannwarth, F. Tuczek, R. Berndt, *Angew. Chem. Int. Ed.* **2012**, *51*, 6262–6266; *Angew. Chem.* **2012**, *124*, 6367–6371.
[17] T. Miyamachi, M. Gruber, V. Davesne, M. Bowen, S. Boukari, L. Joly, F. Scheurer, G. Rogez, T. K. Yamada, P. Ohresser, et al., *Nat. Commun.* **2012**, *3*, 938.
[18] B. Warner et al., *J. Phys. Chem. Lett.* **2013**, *4*, 1546–1552.
[19] S. Shi et al., *Appl. Phys. Lett.* **2009**, *95*, 043303.
[20] T. Palamarciuc, J. C. Oberg, F. E. Hallak, C. F. Hirjibehedin, M. Serri, S. Heutz, J.-F. Létard, P. Rosa, *J. Mater. Chem.* **2012**, *22*, 9690–9695.
[21] M. Gruber, V. Davesne, M. Bowen, S. Boukari, E. Beaurepaire, W. Wulfhekel, T. Miyamachi, *Phys. Rev. B* **2014**, *89*, 195415.
[22] C. Etrillard, V. Faramarzi, J.-F. Dayen, J.-F. Letard, B. Doudin, *Chem. Commun.* **2011**, *47*, 9663–9665.
[23] E. J. Devid et al., *ACS Nano* **2015**, *9*, 4496–4507.
[24] S. Cobo, G. Molnár, J. A. Real, A. Bousseksou, *Angew. Chem. Int. Ed.* **2006**, *45*, 5786–5789; *Angew. Chem.* **2006**, *118*, 5918–5921.
[25] J. A. Real, E. Andrés, M. C. Muñoz, M. Julve, T. Granier, A. Bousseksou, F. Varret, *Science* **1995**, *268*, 265–267.
[26] H. J. Shepherd, T. Palamarciuc, P. Rosa, P. Guionneau, G. Molnár, J.-F. Létard, A. Bousseksou, *Angew. Chem. Int. Ed.* **2012**, *51*, 3910–3914; *Angew. Chem.* **2012**, *124*, 3976–3980.
[27] A. Bousseksou, G. Molnár, L. Salmon, W. Nicolazzi, *Chem. Soc. Rev.* **2011**, *40*, 3313–3335.
[28] C. M. Quintero, G. Félix, I. Suleimanov, J. S. Costa, G. Molnár, L. Salmon, W. Nicolazzi, A. Bousseksou, *Beilstein J. Nanotechnol.* **2014**, *5*, 2230–2239.
[29] E. Ruiz, *Phys. Chem. Chem. Phys.* **2014**, *16*, 14–22.
[30] J. J. Parks et al., *Science* **2010**, *328*, 1370–1373.
[31] V. Meded, A. Bagrets, K. Fink, R. Chandrasekar, M. Ruben, F. Evers, A. Bernand-Mantel, J. S. Seldenthuis, A. Beukman, H. S. J. van der Zant, *Phys. Rev. B* **2011**, *83*, 245415.
[32] M. Ruben, A. Landa, E. Lörtscher, H. Riel, M. Mayor, H. Görls, H. B. Weber, A. Arnold, F. Evers, *Small* **2008**, *4*, 2229–2235.
[33] J. A. Real, A. B. Gaspar, M. C. Muñoz, *Dalton Trans.* **2005**, 2062–2079.
[34] P. Gütlich, Y. Garcia, H. A. Goodwin, *Chem. Soc. Rev.* **2000**, *29*, 419–427.
[35] E. C. Constable et al., *Chem. Eur. J.* **1999**, *5*, 498–508.
[36] D. Aravena, E. Ruiz, *J. Am. Chem. Soc.* **2012**, *134*, 777–779.
[37] H. Häkkinen, *Nat. Chem.* **2012**, *4*, 443–455.
[38] V. V. Zhirnov, R. K. Cavin, *Nat. Mater.* **2006**, *5*, 11–12.
[39] G. D. Harzmann, M. Neuburger, M. Mayor, *Eur. J. Inorg. Chem.* **2013**, 3334–3347.
[40] A. S. Guram, A. O. King, J. G. Allen, X. Wang, L. B. Schenkel, J. Chan, E. E. Bunel, M. M. Faul, R. D. Larsen, M. J. Martinelli, et al., *Org. Lett.* **2006**, *8*, 1787–1789.
[41] The use of freshly prepared solutions is crucial due to the isomerization of the heteroleptic $[Fe^{II}(tpy)_2]$ complexes in acetonitrile. For a 0.5 mM solution of complex **1** in CH_3CN at room temperature, 25% degraded to the homoleptic $[Fe^{II}(tpy)_2]$ complexes **1b** and **1c** within 24 h. Details concerning the isomerization studies are provided in the Supporting Information (page SI-24).

Received: June 13, 2015
Revised: July 16, 2015
Published online: October 1, 2015

